

THESIS FOR THE DEGREE OF LICENTIATE OF ENGINEERING

Investigation of HEV Li-ion Batteries for Lithium Recovery

SRAVYA KOSARAJU



Department of Chemical and Biological Engineering
CHALMERS UNIVERSITY OF TECHNOLOGY
Göteborg, Sweden 2012

Investigation of HEV Li-ion Batteries for Lithium Recovery SRAVYA KOSARAJU

©SRAVYA KOSARAJU 2012

Licentiatavhandlingar vid Chalmers tekniska högskola

Series no: 2012:19

ISSN 1652-943X

Industrial Materials Recycling

Department of Chemical and Biological Engineering

Chalmers University of Technology

SE-412 96 Göteborg

Sweden

Telephone +46 (0)31-772 1000

Chalmers Reproservice

Göteborg, Sweden 2012

Investigation of HEV Li-ion Batteries for Lithium Recovery

SRAVYA KOSARAJU

Industrial Materials Recycling
Department of Chemical and Biological Engineering
Chalmers University of Technology

ABSTRACT

Automobile electrification is one of the technological developments that may establish an eco-friendly transport system by mitigating vehicle emissions, and hopefully lead to a less fossil fuel-dependent society. Conservative forecasts predict four million electric cars on the road by 2015 (Bernhart et al., 2012). A crucial component of electric vehicles is the battery. This component affects two key performance factors, energy storage and usage. This implies that battery performance is the basis for public acceptance of electric vehicles. The lithium-ion (*Li*-ion) battery chemistries are the most popular battery chemistries to fulfill this requirement (especially for the complete electric vehicles) among manufacturers. The large influx of HEVs and EVs will present unique challenges for the safe disposal and recycling of their batteries at the end of product life. The high energy density, ironically the characteristic that makes the Li-ion batteries ideal for electric drive, is the cause for concern in handling and processing them at their end of life.

However, recycling end-of-life batteries for their constituent metals has multifold advantages. If successful, recycling may effectively mitigate environmental effects of mining/brine extractions for virgin metals and raw material transportation emissions. In addition, it can also balance fluctuating cost dynamics and ensure a steady supply of raw material.

Leaching and separation of the metals in the leachates are two of the main steps in a hydrometallurgy process. Mastering these two steps will allow for the possibility to develop a successful process for the recovery of metals e.g., *Li*, *Cu*, *Al*, *Ni*, and *Mn*.

In this work, characterizing of the electrochemically active material on the electrodes in relation to their chemical composition and physical phases using XRD, SEM coupled with EDX was done. Leaching study showed that the state of battery charge or microstructure did not affect leachability of metals from the electrodes. Preliminary solvent extraction experiments using the extractants (Cyanex 272, Cyanex 923 and HDBM) resulted in successful separation of *Li* from other metal ions from chloride solutions.

KEYWORDS: *Li*-ion battery recycling, *Li* recovery, Characterization, *LiFePO₄* electrode, Dissolution study, Solvent Extraction

LIST OF PUBLICATIONS

This thesis is based on the work presented in the following papers:

PAPER I

Kosaraju S., Ekberg C., Allard S. Automotive scale *LiFePO₄/C* battery characterization and metal recovery process.
Manuscript

Contribution

All experimental work, data treatment and evaluation and major part of writing of the manuscript

Contents

1	Introduction	1
1.1	Objective	3
2	The <i>Li</i>-Ion Battery and Recycling Processes	5
2.1	The Vehicle Scale <i>Li</i> -ion Battery Construction	5
2.2	The Working of an <i>Li</i> -Ion Cell	8
2.3	Various Recycling Steps and Methods	8
2.3.1	Hydrochemical methods	9
2.3.1.1	Physical Separation	9
2.3.1.2	Leaching	9
2.3.1.3	Solvent Extraction	9
2.3.2	Pyro-chemical Methods	12
2.3.3	Electrowinning	12
2.3.4	Commercial Recycling Processes	14
3	Materials and Methods	15
3.1	Batteries	15
3.1.1	Battery Chemistry I	15
3.1.2	Battery Chemistry II	16
3.2	Chemicals	16
3.3	Methods	18
3.3.1	Analysis of Surface Area by Gas Adsorption	18

3.3.2	SEM	18
3.3.3	XRD	18
3.3.4	Inductively coupled Plasma Optical Emission Spectrometer (ICP-OES)	19
4	Experiments	21
4.1	Dismantling	21
4.2	Leaching	22
4.3	Batch Solvent Extraction Experiments	22
4.4	Pyro Metallurgical Process	23
5	Results and Discussion	25
5.1	Characterization of <i>LiFePO₄/C</i> Batteries	25
5.1.1	Dismantling and Physical Properties	25
5.1.2	Surface Area Analysis	26
5.1.3	SEM	26
5.1.4	XRD	29
5.2	Leaching	30
5.3	Solvent Extraction	32
5.3.1	Battery Chemistry I	32
5.3.2	Battery Chemistry II	33
5.4	Pyrolysis	36
5.5	Process Suggestion	37
6	Conclusions and Future Research	39
6.1	Conclusions	39
6.2	Future Research	40
	Acknowledgments	41
	Bibliography	43

List of Figures

1.1	A Ragone plot of power storage devices (Shin et al., 2005)	2
2.1	(a) Li-ion battery pack from Nissan Leaf Electric Car (Nissan, 2012); (b) A single battery (prismatic construction) by A123 Systems (A123- Systems, 2012);	5
2.2	Schematic of a single Li-ion cell	6
2.3	Various components of a solvent extraction system. The depletion of aqueous phase is shown in an experiment indicative of one done in a sep- aration funnel	10
2.4	Counter current cascade	11
2.5	$MgCl_2 - KCl - LiCl$ phase diagram (Chartrand and Patrice, 2001)	13
3.1	Lewis structure of bis (2,4,4-trimethylpentyl) phosphinic acid (Chemical- Book, 2012)	17
3.2	Lewis structure of TOPO (Chemical-Book, 2012)	17
3.3	Lewis structure of HDBM (Chemical-Book, 2012)	17
4.1	Inside the battery alternate layers of cathodes, anodes and separator re- spectively, (inset) a new battery	21
4.2	Vertical tube furnace with controller below	23
5.1	(a) SEM image of FB - Anode (electrochemically active material), mag- nification 5000X; (b) SEM image of SB - Anode (electrochemically ac- tive material), magnification 5000X;	28

5.2	(a) SEM image of FB - Cathode (electrochemically active material), magnification 5000X; (b) SEM image of SB - Cathode (electrochemically active material), magnification 5000X;	28
5.3	X-Ray diffractogram of the anode powder indicating peaks (O) match to carbon	29
5.4	X-Ray diffractogram of the FB cathode powder indicating powder indicating peaks of LiFePO_4	29
5.5	SB Cathode powder X-Ray diffractogram indicating a match to LiFePO_4 Orthorhombic structure alongside other peaks	30
5.6	Elemental content of H_2SO_4 leachate FB cathode compared with that of SB at various molarities	30
5.7	Elemental content of HCl leachate FB cathode compared with that of SB at various molarities	31
5.8	Elemental content of HNO_3 leachate FB cathode compared with that of SB at various molarities	31
5.9	%E vs. pH in aqueous media with <i>Li</i> and <i>Fe</i> in chloride media and Organic solvent with Solvent 70 as diluent and Cyanex 272 (5%vol) as extractant	32
5.10	%E vs. pH in aqueous solution with <i>Li</i> , <i>Ni</i> and <i>Mn</i> in chloride media and Organic solvent with Solvent 70 as diluent and Cyanex 272 (5%vol) as an extractant	33
5.11	%E vs. pH in aqueous solution with <i>Li</i> , <i>Ni</i> and <i>Mn</i> in sulfate media and Organic solution with Solvent 70 as diluent and Cyanex 272 (5%vol) as an extractant	34
5.12	%E vs. pH in aqueous solution with <i>Li</i> , <i>Ni</i> and <i>Mn</i> in chloride media and Organic media with Xylene as diluent and Cyanex 923 (5%vol) and HDBM (0.1M) as extractants	35
5.13	Acid leaching of the cathode sample oxidized at 200°C different molarities	36
5.14	Acid leaching of the cathode sample oxidized at 400°C different molarities	36
5.15	Acid leaching of the cathode sample oxidized at 500°C different molarities	37

LIST OF FIGURES

5.16 Acid leaching of the cathode sample oxidized at 600°C different molarities	37
5.17 Suggested process plan	38

List of Tables

2.1	Popular electrode materials for anodes and their respective theoretical capacities (Zhang, 2011)	7
2.2	Popular electrode materials for cathodes and their respective capacities (Zhang, 2011)	7
5.1	Measured physical parameters of the electrodes and the complete battery .	26
5.2	Gas Adsorption analysis of the surface of the anodes of the batteries FB and SB	27

Chapter 1

Introduction

Emission-free transport and fossil fuel-free engines are the current trend for the global automotive industry. This has made hybrid electric vehicles (HEVs) and electric vehicles (EVs) (Karden et al., 2005; Ekeremo, 2009) one of the fastest growing segments of the car market today (Bernhart et al., 2012). Conservative forecasts predict four million electric cars on roads by 2015 (Bernhart et al., 2012). The HEV/EVs require batteries that have high capacity and high energy density (Karden et al., 2005; Gosden, 1993). These batteries also need to have a reversible cell-chemistry with minimal structural deterioration, due to the continuous cycle of charge and discharge. The reversible cell-chemistry is made possible by the introduction of electrodes that undergo charge/discharge cycles, without any significant loss of capacity (Gosden, 1993).

For over a decade now *Li*-ion batteries have been used increasingly for powering device-scale electronics (Pistoia and Gianfranco, 2005). At present they are also the popular choice for vehicular batteries because of their high energy density (Figure 1.1), low self-discharge, long cycle life, almost no maintenance, negligible memory effect, possibility of miniaturization and very thin form factors (Pistoia, 2009). In addition, the specific energy varies between $100Wh(kg)^{-1}$ and $150Wh(kg)^{-1}$ depending on the electrode active materials structure (Scrosati and Garche, n.d.). The newer thin film *Li*-ion batteries have reported a range of $300 - 500Wh(kg)^{-1}$ (Patil et al., 2008). The large influx of HEVs and EVs, present unique challenges for the safe disposal and recycling of the batteries at the end of product life (Gaines, 2009).

According to the European directive 2006/66/EC, 95% by weight of a car must be recycled for recovery and reuse from January 2015 (Parliament and the council of the European Union, 2006). Resource availability is a constraint to be taken into consideration for product manufacturing. In the case of *Li*-ion battery, *Li* availability and control over brines has been a subject of much controversy in recent times (Tahil, 2008; Yaksic and Tilton, 2009). The price of *Li* compounds has recently shown a steady increase (Grosjean

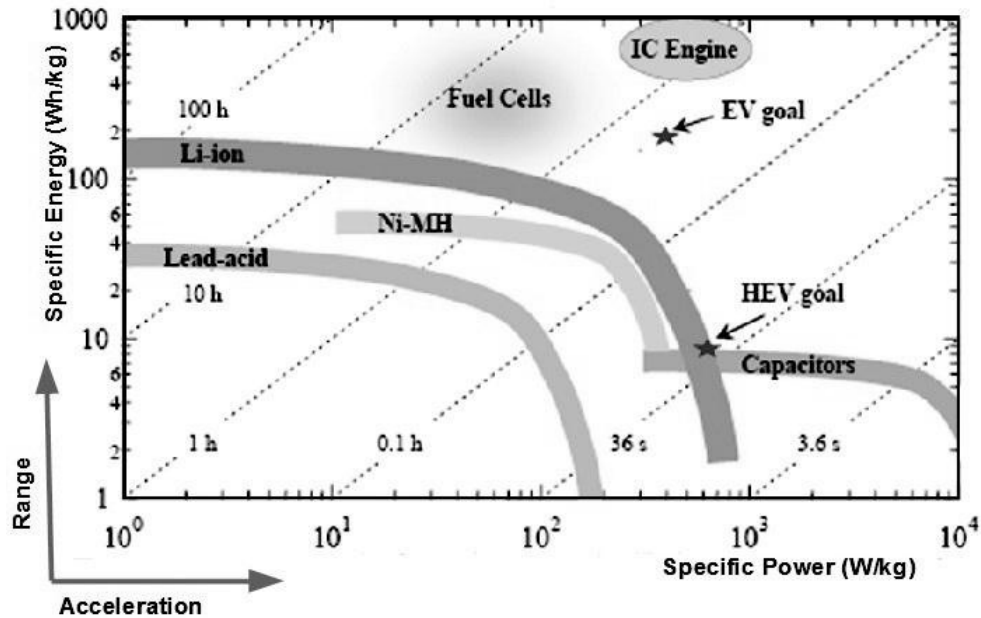


Figure 1.1. A Ragone plot of power storage devices (Shin et al., 2005)

et al., 2012). About 40% of the battery cost is that of the cathode (Grosjean et al., 2012). However, *Li* is not as expensive (price/weight) as the other metals in batteries. At present, prices of other metals used within the battery such as *Cu*, *Al*, *Ni*, *Mn* play a more significant role in the cost of manufacturing of the battery. This leaves little motivation for *Li* recovery; hence *Li* ends up as slag/waste in all commercial recycling facilities at present.

Recycling should not be viewed only in terms of economic viability as it is often today, but also in terms of the larger picture, including future material constraints. If successful, recycling may effectively mitigate environmental effects of mining/ brine extractions for virgin metals, raw material transportation emissions. In addition it can also balance fluctuating cost dynamics and ensure a steady supply of raw material.

However, there is a general reluctance among the manufacturing industries to re-use the recycled product due to the possibility of impurities compromising the performance of the final product. The objective of metal recovery is not fulfilled if the purity of the recovered metals is not comparable to that of the metals used in the manufacture of new products. Resource analysts report that commercial recycling systems hardly create pure material streams, especially in the vehicle waste related stream, because waste is treated not depending on the metal fractions of the weight but as a universal set of waste (Reuter et al., 2006).

1.1 Objective

The aim of this project is to concentrate on *Li* extraction, along with other important metals from ELBs from HEVs and EVs, their respective production discards and secondary waste during manufacture. It is an attempt to develop a process which recovers all metal fractions at high purity so they can at least partially replace virgin metals in the manufacturing of new batteries. Economic viability and sustainability in terms of energy and time will also be addressed.

The focus of this thesis is to investigate the *Li*-ion batteries at different physical end-of-life states simulating the real conditions at the battery recycling facility. This is specifically done by surface and phase characterizations, and acid dissolution studies. This study optimizes conditions to pretreat batteries before metal separation and purification. A preliminary study on the possibility of *Li* extraction using hydrometallurgical process was also investigated.

Chapter 2

The *Li*-Ion Battery and Recycling Processes

2.1 The Vehicle Scale *Li*-ion Battery Construction

The EV/HEV battery has a number of *Li*-ion batteries connected in parallel or series or both according to the power requirement and the wattage of the battery. This is usually termed as a 'battery pack' (Figure 2.1(a)). The prismatic construction of the *Li*-ion battery (shown in Figure 2.1(b)) is among the more popular constructions for the vehicle scale batteries. A single *Li*-ion battery (Figure 2.1(b)) is composed of several *Li*-ion cells (Figure 2.2).

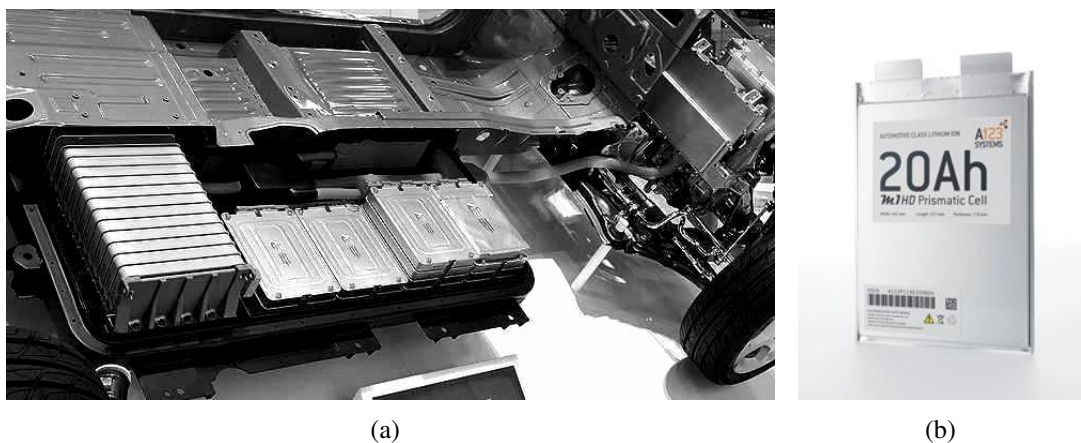


Figure 2.1. (a) Li-ion battery pack from Nissan Leaf Electric Car (Nissan, 2012); (b) A single battery (prismatic construction) by A123 Systems (A123-Systems, 2012);

The main components of an *Li*-ion cell (like most batteries) are anode, cathode, separator

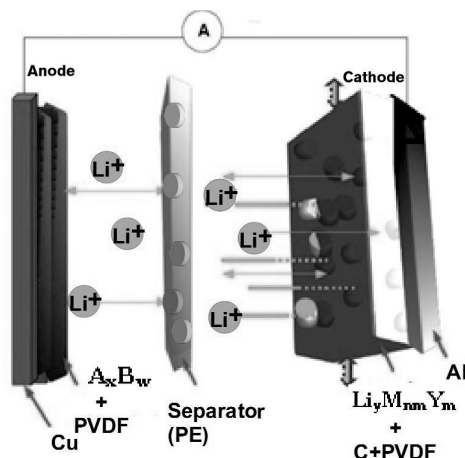


Figure 2.2. Schematic of a single Li-ion cell

(plastic such as PE), electrolyte, the cell container and terminals. Both anodes and cathodes are composites i.e., the electrochemically active materials that are attached to current collectors which are metallic substrates usually made of, e.g., *Cu* and/or *Al* foils. The adhesion is done with the help of an adhesive such as poly vinylidene di-fluoride (pVdF). The surface is coated with carbon powder to increase conductivity.

In more detail, the principal components of an *Li*-ion cell are:

Anode The negative electrode or the electrode which generates electrons. Carbon based compounds are the most commonly used anode-electrochemically active material at present due to their long cycle life, abundant material supply and relatively low cost (Endo et al., 2000). However, the graphite anode has a disadvantage; low energy density as compared to alloy anodes. Alloy anodes are electrodes which have metallic matrices (one major metal and other inclusions) to allow for *Li*-insertion. The main challenge for the implementation of alloy anodes is their large volume change (up to 300%) during *Li*-insertion and extraction (Zhang, 2011). These materials are still under investigation to improve their structural decay properties. A list of anode active materials in comparison to the theoretical capacities is given in Table 2.1.

Cathode The positive electrode, which has the *Li* compound as the active material. (*LiMY* is chosen as the notation in the equations below to imply metallic oxides, phosphates or silicates, which are some of the popular chemical forms used for active materials in *Li*-ion batteries). As this electrode is the *Li* bearing one, it is focus of the experiments in this thesis. A list of cathode active materials is given in Table 2.2.

The general usage of a battery is during battery discharge. This convention is used to label carbon and *Li*-compounds as anode and cathode respectively. It should be noted that while charging this notation is reversed.

Table 2.1. Popular electrode materials for anodes and their respective theoretical capacities (Zhang, 2011)

Anode	Theoretical Specific Capacity (mAh/g)
Carbon based	
Spherical graphitized mesocarbon microbeads (MCMB)	320-330
Graphitized carbon fibre	360-365
Carbon coated natural fibre	360-380
Alloy	
<i>Li</i>	3862
<i>Si</i>	990
<i>Sn</i>	4200
<i>Al</i>	990
<i>Sb</i>	650
<i>Mg</i>	3350
<i>Bi</i>	385

Different electrochemically active materials for the anode and cathode are shown in Table 2.1 and Table 2.2 together with their respective capacities. The capacity of a battery is the amount of energy a battery can store and is measured in ampere*hours(Ah) (Gosden, 1993). The values seen in the tables are specific gravimetric capacities hence the unit battery can store and is measured in . The values seen in the tables are gravimetric capacities hence the *mAh/g*.

Table 2.2. Popular electrode materials for cathodes and their respective capacities (Zhang, 2011)

Cathode	Practical Capacity (mAh/g)
<i>LiCoO₂</i>	160
<i>LiMn₂O₄</i>	110
<i>LiFePO₄</i>	160
<i>LiNi_{0.5}Mn_{0.5}O₂</i>	200

Electrolyte The medium that enables ion movement from cathode to anode and vice versa. The electrolytes are usually made by dissolving *Li* salts such as *LiPF₆* in an aprotic solvent such as ethylenecarbonate (EC), propylenecarbonate (PC), dimethylcarbonate (DMC), diethylcarbonate or their mixtures, but many other solvents and salts

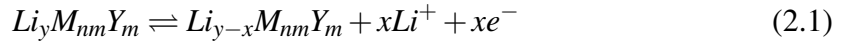
may be used for this purpose. The choice of the salt-solvent combination will determine important properties such as the conductivity, and the thermal and electrochemical stability of *Li*-ion cells.

2.2 The Working of an *Li*-Ion Cell

The *Li*-ion cell is a secondary cell/ is re-chargeable because of its ability to let the *Li*-ion move from anode to cathode and back again. Such reversible cell chemistry with minimal structural disintegration, due to the cycle of charge and discharge is possible due to electrodes designed to be intercalate-able. An intercalation process is a reversible chemical reaction in which the guest species occupy empty sites in a solid structure in such a way that the initial and final lattices of the electrode are in coherent reaction with the guest species (Broussely et al., 1999). It should be noted that the core crystal structure never changes but the orientation of the outer stacked atoms (usually oxygen atoms) is shifted during the insertions and extractions of *Li*-ions.

The working of *Li*-ion cell is demonstrated by the schematic in Figure 2.2. Their respective half-cell (or charge-discharge) reactions are as following.

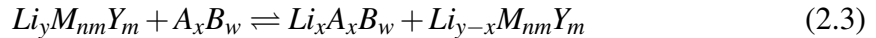
At the cathode,



At the anode,



The overall cell reaction,



2.3 Various Recycling Steps and Methods

The following processes are steps in a recycling process and are combined to make a complete recycling process. However sometimes these processes may be used as full recycling processes by themselves. Some of them have been commercially established. The first step is dismantling and separation of the packaging, to reach the chemically reactive substances, usually the anode, cathode, electrolyte and (sometimes) the separators. For hydrochemical methods, after dismantling, various methods of metal separation and recovery follow.

2.3.1 Hydrochemical methods

2.3.1.1 Physical Separation

Physical processes for recycling include any mechanical processes for the separation of electrodes from separators, terminals, and the outer case. An inert and dry atmosphere is suitable for mechanical processing of the batteries, as it avoids exposing the cell contents to water vapor which can react with metallic Li formed inside the battery due to cycling. It also reduces the impact of internal short-circuiting during dismantling, leading to fast hydrogen gas production from the electrolyte. This can be a violent reaction when in contact with oxygen (Gaines, 2009). Mechanical processes involve crushing, sieving, magnetic separation, fine crushing and classification to yield a concentrated material for recovery using other processes. Mechanical separation done before leaching process usually improve the recovery efficiency of target metals and eliminates the need for a purification process of the leachate.

2.3.1.2 Leaching

Leaching is a method by which the metal constituents in the battery electrodes can be dissolved into an aqueous media. For this purpose mainly oxidizing acids are used. In the case of *Li*-ion batteries, since the electrodes have organic adhesives, few processes use organic solvents to dissolve the adhesive. When the adhesive dissolves, electrode particles are separated from the rest, i.e., substrates *Cu/Al* and plastic separators. The metal containing fractions are then dissolved using acids.

2.3.1.3 Solvent Extraction

Solvent extraction / liquid-liquid distribution is the distribution of a solute between two liquids that must not be completely mutually miscible (Choppin et al., 2004). The aqueous phase in solvent extraction system is often the leachate from the previous hydrometallurgy process. This means that the selection of dissolution process must be done carefully so as to not cause problems in the solvent extraction process. In most extraction systems the organic phase is comprised of one or more extractants in a diluent. The diluent and the extractant together make a solvent.

A solvent extraction system in a separation funnel is shown in Figure 2.3(left). The metal rich aqueous phase is in contact with an immiscible diluent phase. After mixing the two liquids thoroughly and letting them settle, the solute species distributes themselves between the two immiscible liquids. Most processes are designed to extract the desired element into the organic phase, However in some cases it is more advantageous to extract

all metals except the desired one. If the aim is to extract the desired element to the organic phase, this phase is said to be ‘pregnant’ and the aqueous phase is said to be ‘depleted’ of the solute species. The distribution of the solute species can be manipulated by many factors such pH, temperature, type of solvent, type of extractant, the counter ion in aqueous media and all of their respective concentrations

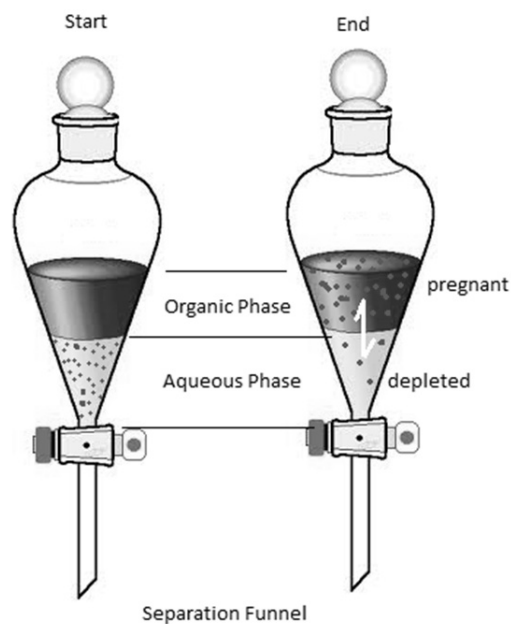


Figure 2.3. Various components of a solvent extraction system. The depletion of aqueous phase is shown in an experiment indicative of one done in a separation funnel

The schematic of various components of solvent extraction and separation is described in Figure 2.3. The distribution ratio (D) and percentage extraction ($\%E$) of the metal ion are the factors of interest in these experiments.

The distribution ratio is defined as the ratio between the total analytical concentrations of the species in the organic phase $[C]_{org}$ divided by the total analytical concentration of a species in aqueous phase $[C]_{aq}$.

Distribution ratio is given by,

$$D = \frac{[c]_{org}}{[c]_{aq}} \quad (2.4)$$

Θ is the ratio of the volumes of organic phase V_{org} and volume of aqueous phase V_{aq}

given by,

$$\Theta = \frac{[V]_{org}}{[V]_{aq}} \quad (2.5)$$

and the percentage extraction is given by,

$$\%E = \frac{(100 * D)}{(1 + D)} \quad (2.6)$$

The selectivity of extractive separations of metal ions M^{n+} is commonly described by the separation factor (SF), defined as the ratio of the distribution ratios of the ions in the same system, e.g. M_1 and M_2 , shown in equation 2.6.

$$SF = \frac{D_{M1}}{D_{M2}} \quad (2.7)$$

For industrial processes usually a countercurrent extraction flow scheme (Figure 2.4) is used because of greater efficiency of the process (the phase volumes remain constant and by feeding the two phases aqueous and organic, at opposite ends, the driving force for extraction i.e., the solute concentration difference between the two phases is maximized (Choppin et al., 2004)). The concentrations of feed and raffinate are represented by x_f and x_n in aqueous and y_f and y_n in organic phases.

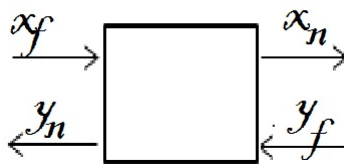


Figure 2.4. Counter current cascade

The extraction factor is given by,

$$P = \Theta * D \quad (2.8)$$

where D is the distribution factor (equation 2.4), and Θ is the ratio of volume of phases (equation 2.5).

For multi-step extraction,

$$x_n = x_f \frac{P - 1}{P^{n+1} - 1} \quad (2.9)$$

where n is the number of stages.

Charged or hydrated compounds such as dissolved metal ions are not soluble in most organic solvents. Thus, in order to extract metals to organic phase (like-dissolves-like rule). Specialized organic molecules (extractants) are used to form different types of complexes with the metal ion before they can be extracted. Depending on the reaction mechanism, the extractants can be classified mainly as (Marcus, 1979),

Acidic The organic acid dissociates, and its conjugated base reacts with metal cation to form a neutral complex.

Basic/ion pair Forms an ion pair with negatively charged metal complex in the aqueous phase.

Solvating Extractant forms an adduct with coordinately unsaturated metal ligand complex by replacing coordinated water molecules.

2.3.2 Pyro-chemical Methods

Pyro-chemistry involves the incineration/melting of used batteries at high temperatures in a furnace with controlled atmosphere. Ar atmosphere is usually the preferred atmosphere for *Li*-ion batteries as molten *Li* reacts exothermically with nitrogen gas. The metallic constituents then form alloys while the organic constituents burn off. The ventilation of these burnt organic fractions needs to be carefully dealt with since they may contain fluoride compounds.

The metal solution/alloy needs to be further processed to recover specific metals. This may require acidic leaching or electro-metallurgical techniques such as molten salt electrowinning. Pyro-chemical methods need high energy input, due to the high temperatures required to melt all the contents of a battery. In addition, pyro metallurgical processes can be potentially dangerous for vehicle-scale *Li*-ion batteries since their constituents can be explosive at higher temperatures. In addition, since the battery is melted as whole, it might be difficult to separate the metals in to pure fractions.

2.3.3 Electrowinning

Electrowinning is usually a secondary purification process to be utilized either in combination with hydro and or pyro-chemical recycling processes. The process involves pass-

ing electric current through the electrolyte (eluate). Electrons (electricity) pass from the cathode (negative electrode), through the solution and into the anode (positive electrode), completing the electrical circuit. The current causes the metal ion to reduce and to plate on cathodes. In case of *Li*, electrowinning from aqueous electrolyte is not efficient because hydrogen reduction occurs at higher potential than *Li* (-3.05V compared to 0.0V at 25°C for standard state conditions). Instead to obtain pure metallic *Li*, (or sometimes compounds like LiO_2 , LiCl , or Li_2S) electrowinning from molten salts is done. In molten salt extractions, a eutectic mixture such as $\text{KCl} - \text{MgCl}_2$ is used in place of an electrolyte. The molten salt is chosen so that eutectoid point for all three components is much lower than the individual melting point of its constituents. The phase diagram of $\text{MgCl}_2 - \text{KCl} - \text{LiCl}$ (Figure 2.5) shows that the eutectoid temperature is 421°C . While slightly above that temperature, pure LiCl can be extracted at an appropriate mole fraction. Using electrowinning, very pure metals or their compounds can be produced in their crystalline form. This product does not often require more refining.

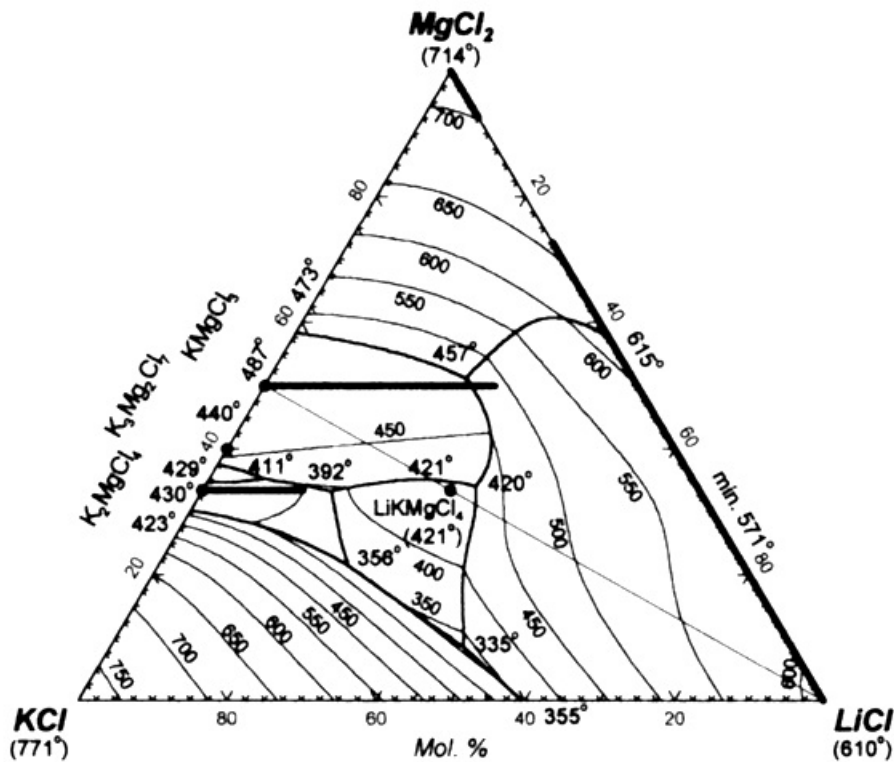


Figure 2.5. $\text{MgCl}_2 - \text{KCl} - \text{LiCl}$ phase diagram (Chartrand and Patrice, 2001)

2.3.4 Commercial Recycling Processes

Most of the previous work in recycling of *Li*-ion batteries has been mainly in the context of device scale batteries, also mainly for the recovery of economically more viable metals such as *Cu, Co, Ni, Mn* (Ekeremo, 2009). Owing to the economic non-viability attitude, *Li* ends up either as slag or as a secondary product along with several other process impurities. Industrial recycling facilities Accurec GmbH, Falconbridge International Ltd., Sony (Bernardes et al., 2004) use pyro-metallurgical processes mainly to recover *Cu, Al, Co, Mn*, but *Li* is only recovered only either as impurity in the above metal/alloy fractions or in slag. Toxco Inc. uses a hydrometallurgical process concentrating on *Ni, Cu, Co* recovery (Inc., 2012). Umicore's Val' Eas process is also a pyro-metallurgical process combined with hydrochemical methods for recovery of *Ni* and *Cu* and would not be viable for *Li*. There are two established recycling processes for *Li*-ion cells and batteries, using higher temperatures to recover *Co* and *Ni* (Pistoia and Gianfranco, 2005). All the commercial facilities listed above currently handle device scale *Li*-ion batteries, which do not have the same safety issues as with the automotive scale which are both larger and have high energy.

Chapter 3

Materials and Methods

3.1 Batteries

In the course of this project, the HEV Li-ion batteries used for experimentation are provided by ETC Battery and Fuels Cells Sweden AB. Parts of the experiments are also done by making stoichiometric solutions based on an ongoing EU- battery project under the 7th Framework Program called 'APPLES'.

3.1.1 Battery Chemistry I

The 'ETC Battery' has the following components:

Cathode	<i>LiFePO₄</i> Carbon Black PVDF Al foil
Anode	Graphite Carbon Black PVDF Cu foil
Electrolyte	Di-Ethyl Carbonate (DEC) Ethylene Carbonate (EC) <i>LiPF₆</i>

3.1.2 Battery Chemistry II

The APPLES battery has the following components:

Cathode	$LiNi_{0.5}Mn_{1.5}O_4$ Carbon Black Al foil PVDF
Anode	Sn-C Carbon Black PVDF
Electrolyte	EC DEC PVDF

3.2 Chemicals

The chemicals used for metal dissolution for characterization were hydrochloric acid (puriss, 37%, Sigma-Aldrich), nitric acid (puriss, 69%, Sigma-Aldrich), sulfuric acid (95%purity, Acros Organic) and MilliQ water ($> 18M\Omega$). The samples for measuring were prepared by diluting the leachate samples in 1.5M HNO_3 (puriss, 69%, Sigma-Aldrich) and MilliQ water ($> 18M\Omega$).

The electrolyte for electrolysis experiments was made from Ethylene carbonate (98%, Sigma-Aldrich), Di methyl carbonate ($\geq 99\%$, Sigma Aldrich), $LiPF_6$ (98%, Sigma-Aldrich).

To make stock solutions representing APPLES battery for solvent extraction batch experiments, $Li_2SO_4 \cdot H_2O$ (99% Riedel-Detlaen), LiCl (98% Extrapur, Scharlau Chemie), $NiCl_2 \cdot 6H_2O$ (98% Sigma Aldrich), $NiSO_4 \cdot 6H_2O$ (99% Analyti grade, Merck), $MnCl_2 \cdot 4H_2O$ (99.9% Sigma Aldrich), $MnSO_4 \cdot H_2O$ (Pro Analyti grade, Merck) were used.

For solvent extraction studies, Cyanex[®] 272, Cyanex[®] 923 extractants from Cytec was used. Cyanex 272 is an acidic extractant whose active component of Cyanex 272 extractant is bis(2,4,4-trimethylpentyl) phosphinic acid, shown in Figure 3.1.

For the organic solvent, Solvent 70 (0.5% aromatics, StatOil), and Cyanex 272, Cyanex 923 extractants from Cytec was used.

Cyanex 272 is an acidic extractant whose active component is bis(2,4,4-trimethylpentyl) phosphinic acid (Figure 3.1).

Cyanex 923 is a solvating extractant. The active component is a mixture of four tri-alkyl-phosphine oxides comparable to that of the more conventional extractant TOPO, shown

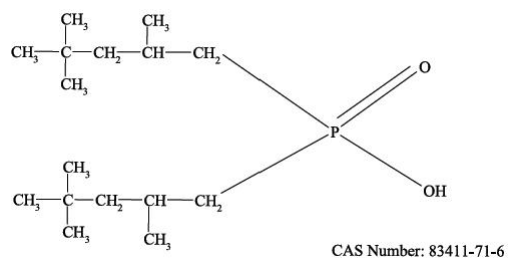


Figure 3.1. Lewis structure of bis (2,4,4-trimethylpentyl) phosphinic acid (Chemical-Book, 2012)

in Figure 3.2.

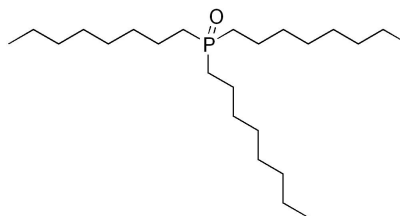


Figure 3.2. Lewis structure of TOPO (Chemical-Book, 2012)

Dibenzoyl methane (1,3-diphenyl-1,3 propanedione) or HDBM was also used as an extractant as it was reported to extract Li (Lee et al., 1968). The Lewis structure is shown in Figure 3.3.

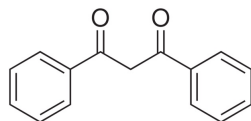


Figure 3.3. Lewis structure of HDBM (Chemical-Book, 2012)

3.3 Methods

The analysis methods used are described below.

3.3.1 Analysis of Surface Area by Gas Adsorption

The surface area (BET) and porosity measurements (BJH) were done using Micrometrics ASAP2020-accelerated surface area and porosimetry system and nitrogen gas. Measuring the surface was done to better understand the surface changes due cycling or shortcircuiting.

This method is based on the physical adsorption of gases on the external and accessible internal surfaces of a porous material. The material is surrounded by and in equilibrium with the measuring gas at a constant temperature. The amount of adsorbed gas depends on its relative vapor pressure and is proportional to the external and internal surface of the material.

Before performing the experiments, the active materials from the anodes of the samples were scraped off from the current collectors, and made solvent free by placing in an oven at 60°C for 24 hours.

3.3.2 SEM

For micro-structure study and elemental analysis, FEI Quanta 200 ESEM FEG with an Oxford Inca 300 Energy dispersive X-ray (EDX) system and a Siemens D5000 diffractometer were used. SEM images give details about morphology of the samples. FEI Quanta 200 ESEM FEG with an Oxford Inca 300 Energy dispersive X-ray (EDX) system was used for chemical analysis. Images were taken mainly with 15kV operating voltage in high vacuum mode. The EDX results were not however used in the thesis because the lithium peak cannot be measured as Li X-ray beam intensity is above its detection limit.

3.3.3 XRD

Siemens D5000 diffractometer, employing *Cu K α* source and a scintillation detector was used to determine the crystal structure of anode and cathode surface films of both FB and SB. This was done to check if it is the same active material when short circuited or if the Li migrates to the extent of changing the compound.

3.3.4 Inductively coupled Plasma Optical Emission Spectrometer (ICP-OES)

A thermo iCAP 6500 ICP-OES was used to measure the elemental composition of the samples taken from the leaching experiments above.). The ICP-OES works on the principle of plasma excitation of atoms and detecting emitted light from the relaxation of the excited atoms. Each element has a unique set of spectral lines and can thereby be detected individually in the same sample. The intensity of the emitted light at a certain wavelength is then correlated to the intensity measured from standard concentration samples, with care taken to avoid interferences and matrix effects.

Chapter 4

Experiments

4.1 Dismantling

Two batteries of the battery chemistry-1 (Chapter 3) were studied, one of which was a non-cycled fresh battery (FB), and the other was short-circuited while cycling (SB). The non-cycled battery, FB, was first discharged slowly from 3.9 volts to 2.3 volts before dismantling. Both batteries FB and SC were then dismantled in a fume hood. The Al-polymer pouch was cut open at a corner and vented for few minutes. The electrolyte vaporized quickly. The electrodes which were then originally neatly stacked with polythene sheets in between were separated (Figure 4.1). The individual anode and cathode pages were separated.



Figure 4.1. Inside the battery alternate layers of cathodes, anodes and separator respectively, (inset) a new battery

The various physical parameters such as length, width, weight of the electrodes were measured. One anode and one cathode from each battery was taken and immersed in water and shaken for 30 minutes and the electrochemically active layers were separated from the substrate metals (*Cu* and *Al*). Both the fractions- substrate metal and electrochemically

active fractions were separated by filtration, dried and masses measured.

4.2 Leaching

The *Li* containing electrodes are the cathodes and the XRD analysis and initial substrate separation by dipping it in liquid (discussed in results) confirmed that the amount *Li* that migrated on to the anode (about 10%) can be dissolved in the water while substrate removal and the remaining carbon material was devoid of any *Li*. Therefore, cathodes were of primary focus in these experiments. The quantity of *Li* leached using *HCl*, *HNO₃*, *H₂SO₄* concentrations of 1, 2, 3, 4, and 5 molar was investigated. The leaching was checked by sampling repeatedly until the system reached equilibrium. This proved to occur at the maximum of two weeks. The samples were all continuously stirred at 500 rpm with a magnetic stirrer at room temperature ($21 \pm 0.5^\circ\text{C}$). Each experiment was made in triplicate, allowing for an uncertainty analysis. The metal content in the samples from the leaching were then measured using ICP-OES.

A total metal content determination was made by dissolving the samples in aquaregia (3:1 conc *HCl* : conc *HNO₃*).

4.3 Batch Solvent Extraction Experiments

Stock solutions were made based on elemental composition from the acid leaching studies. The organic solvent was Solvent 70 as diluent and the extractants used were Cyanex272 and Cyanex923 (each separately). The mixing was done using a shaking device at 1500rpm for 20 minutes at room temperature ($21 \pm 0.5^\circ\text{C}$). The separation was facilitated by centrifugation at 12000rpm for 10 minutes. The effect of pH was studied by additions of 2M *NaOH*. Samples from the aqueous phase diluted to 0.1 times the original concentration using 1M *HNO₃*, were measured using ICP-OES.

Samples of the organic phase for the *Li – Fe* system were stripped with 1M acid of the same kind of counter ion as used in the aqueous solution and the metal content was measured with ICP-OES. The stripping efficiency was tested by stripping organic samples with 1, 2, and 3M acids of the same type. An *O : A1 : 2* was used to make sure there was complete stripping of the organic phase and for the ease of sampling. It was found that no real gain in stripping was achieved by using higher acidity. For the *Li – Ni – Mn* system, the calculations were made based the measurements made only on the aqueous solutions. The concentration of metal in the organic phase is calculated by the difference of concentration of aqueous phases in the feed and the sample. The assumption is that all metal not found in aqueous phase is in the organic phase.

4.4 Pyro Metallurgical Process

High temperature oxidation studies of the cathode materials were made (at 200, 400, 500 and 600°C) in presence of oxygen. The goal was to investigate the elimination of both carbon and PVDF (binder) by oxidation. The experiments were carried out in a vertical tube furnace shown in Figure 4.2.



Figure 4.2. Vertical tube furnace with controller below

Chapter 5

Results and Discussion

Experiments were done in the order of a potential battery recycling process, i.e. dismantling, acid leaching and solvent extraction. The results presented were made based on the analysis methods such as ICP-OES, XRD, SEM presented in 3.

5.1 Characterization of $LiFePO_4/C$ Batteries

5.1.1 Dismantling and Physical Properties

Both the batteries, non-cycled battery (FB) and short-circuited battery (SB) have similar physical parameters as shown in Table 5.1. The amount of Li in the battery is about 10g.

Pure substrate metal foils were collected on both sides by ultra-sonication in water at room temperature $21 \pm 0.5^\circ C$, for 20 minutes. The mass of water used was not important in this case other than that the volume should be greater than the electrodes themselves to ensure complete immersion. However if the leach water should be used for Li recovery, it should be made as concentrated as possible, by reusing the same water for more electrodes.

For the FB battery, the water was analyzed for Li content. The amount of Li in the water at the cathode was $\leq 5.3\text{mg}/\text{electrode}$. For a complete cell, the amount of Li was estimated to be approximately 212mg. The average amount of Li in water at the anode was approximately $\leq 2.1\text{mg}/\text{electrode}$, and for the complete cell this was approximately 84mg. The SB battery had slightly higher values. The total amount of Li dissolved in water during substrate separation was estimated to about 2-5% of the mass of Li present in the complete cell.

Table 5.1. Measured physical parameters of the electrodes and the complete battery

Cell	The complete cell mass	570g
	Al-polymer cover mass	16g
	Number of Anodes	40
	Number of Cathodes	40
Cathode	Each electrode mass	$\approx 7g$
	Each Cu-substrate mass	$\approx 1.5g$
	Length of each electrode	172mm
	Width of each electrode	120mm
	Thickness of each electrode	0.14mm
	Foil thickness	$< 0.1mm$
	Total mass of all Cathodes	$\approx 295g$
	Total mass of active material	$\approx 237g$
Total mass of substrate (Al)	$\approx 58g$	
Anode	Each electrode mass	$\approx 6g$
	Each Cu-substrate mass	$\approx 4.5g$
	Length of each electrode	172mm
	Width of each electrode	120mm
	Thickness of each electrode	$\approx 0.12mm$
	Foil thickness	$< 0.1mm$
	Total mass of all Anodes	$\approx 240g$
	Total mass of active material(graphite)	$\approx 60g$
Total mass of substrate	$\approx 180g$	

5.1.2 Surface Area Analysis

The surface analysis was made using the BET and BJH gas adsorption techniques (Table 5.2), indicates that the surface area of the SB anode increased relative to that of the FB. The average pore size however decreased while the volume of the pores slightly increased. This may be explained by the formation of SEI (solid electrolyte interphase), a layer of different compounds formed due to the interaction between electrode surface and electrolyte components.

5.1.3 SEM

The SEM pictures of FB anode and SB anode are shown in Figure 5.1. The pictures of FB cathode and SB cathode are shown in Figure 5.2. SEM images showed that the structure of the anode and cathode of the short circuited battery was irrecoverably damaged compared to the non-cycled and properly discharged battery. The SB anode displayed surface crack created due to short-circuiting and discontinuous dendrites compared to FB anode. The

Table 5.2. Gas Adsorption analysis of the surface of the anodes of the batteries FB and SB

Cell type	FB	SB
BET surface area (m^2/g)	2.39 ± 0.01	11.33 ± 0.04
BJH : Cumulative Volume of Pores (cm^3/g)		
Adsorption	0.02 ± 0.009	0.12 ± 0.009
Desorption	0.02 ± 0.001	0.09 ± 0.007
BJH : Average Pore Size (width, Å)		
Adsorption	458 ± 0.4	399 ± 0.9
Desorption	0.02 ± 0.8	290 ± 0.3

SB cathode shows loss of regular granular structure instead seems to be covered with structure less clots. This indicates the formation of solid electrolyte interphase (SEI). Based on the composition of SEI, the extent of leachability or the strength of acid needed to dissolve the SEI may vary. This is an uncertainty with respect to every battery that must be taken in to consideration during acid leaching stage of recycling.

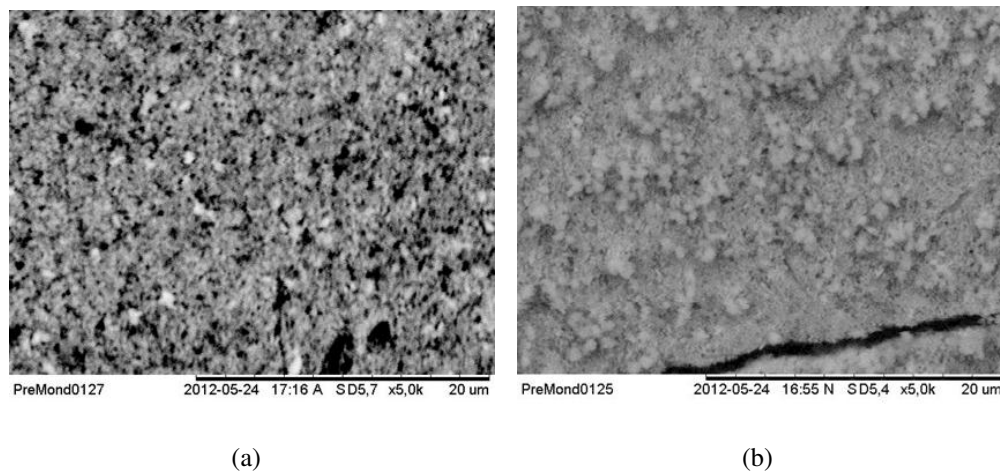


Figure 5.1. (a) SEM image of FB - Anode (electrochemically active material), magnification 5000X; (b) SEM image of SB - Anode (electrochemically active material), magnification 5000X;

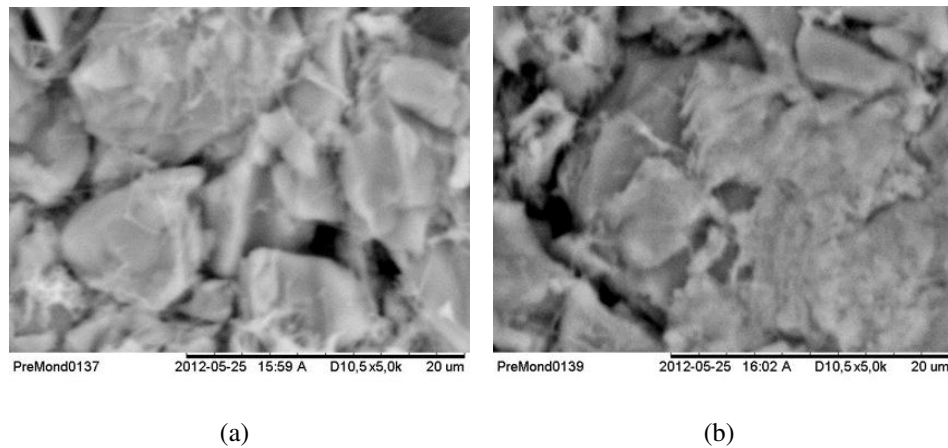


Figure 5.2. (a) SEM image of FB - Cathode (electrochemically active material), magnification 5000X; (b) SEM image of SB - Cathode (electrochemically active material), magnification 5000X;

5.1.4 XRD

The diffractograms for both FB anode and SB anode were identical. Thus only the XRD for FB anode is shown in Figure 5.3. This shows that the microstructure changed due to short-circuiting but not the macro structure. The XRDs of the FB cathode and SB cathode are shown in Figure 5.4 and Figure 5.5.

The diffractogram of the SB had peaks representing other compounds along with those of LiFePO_4 , representative of Li_2O , LiF , confirming the SEI formation as was speculated in the SEM experiments.

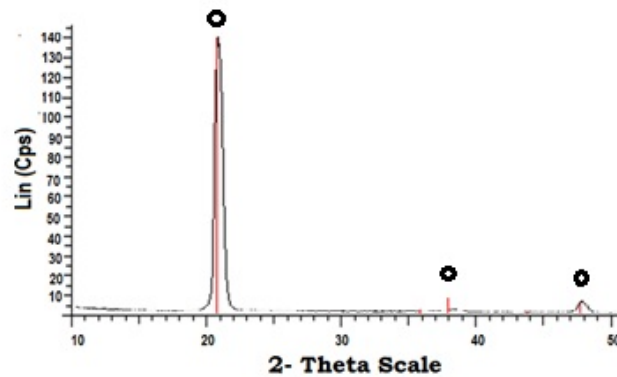


Figure 5.3. X-Ray diffractogram of the anode powder indicating peaks (O) match to carbon

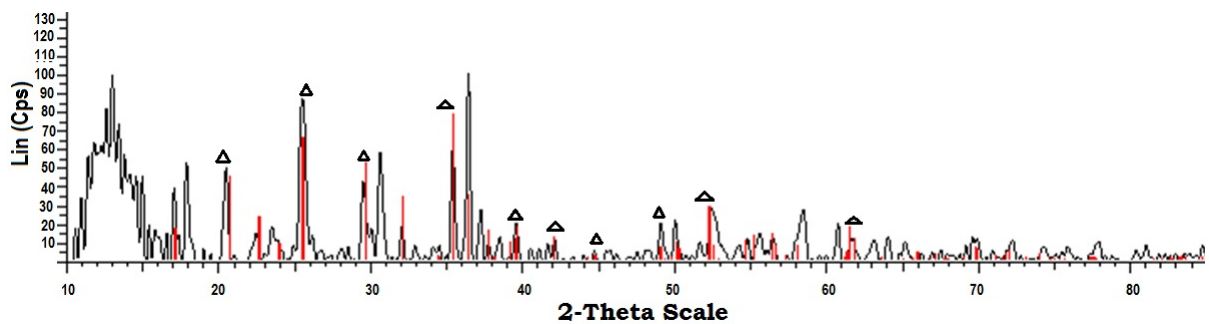


Figure 5.4. X-Ray diffractogram of the FB cathode powder indicating powder indicating peaks of LiFePO_4

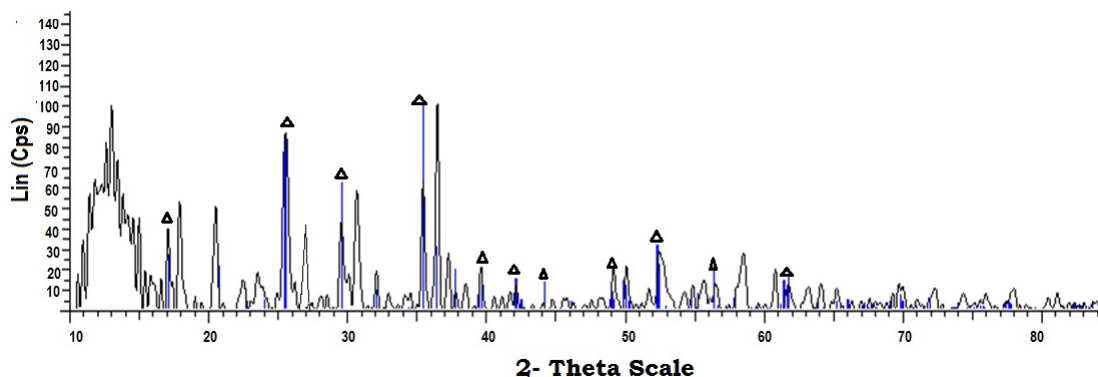


Figure 5.5. SB Cathode powder X-Ray diffractogram indicating a match to $LiFePO_4$ Orthorhombic structure alongside other peaks

5.2 Leaching

The acid leaching studies (figures 5.6, 5.7, 5.8) show that at equilibrium most of the Li and Al can be leached out at rather low acidities together with about 60-70% P and about 50% Fe. There seemed to be no appreciable difference between the different acids used and their Li leachability. More importantly, the state of the battery whether short-circuited or properly discharged did not have any effect on Li-leachability. This proves that the counter-ion for leaching or the state of battery is not an important factor for metal recovery. Each experiment was made in triplicate and the uncertainties are calculated.

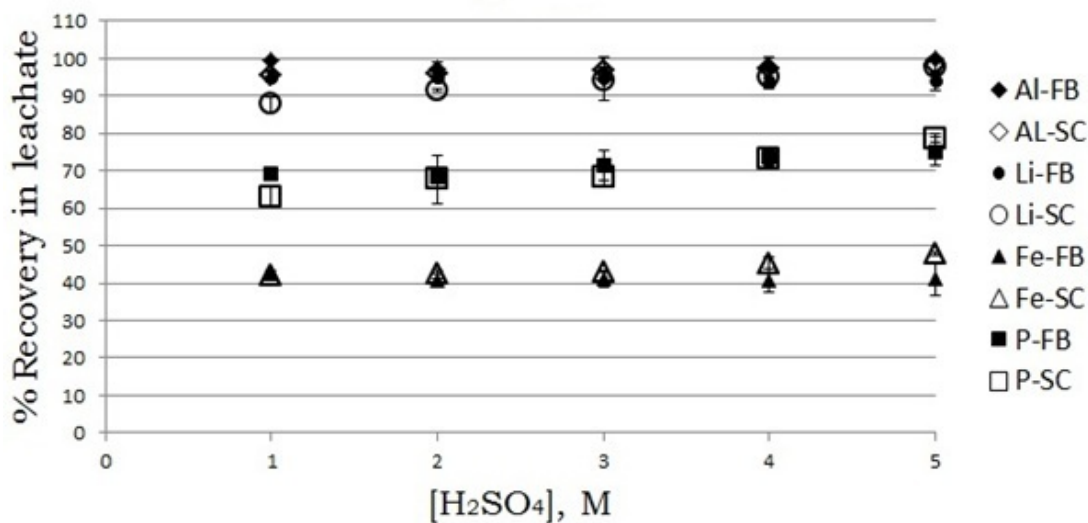


Figure 5.6. Elemental content of H_2SO_4 leachate FB cathode compared with that of SB at various molarities

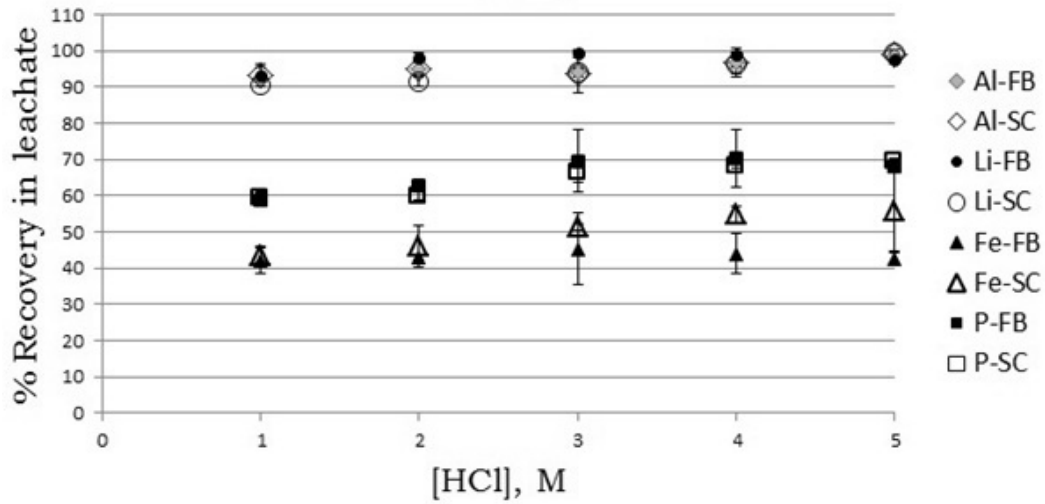


Figure 5.7. Elemental content of HCl leachate FB cathode compared with that of SB at various molarities

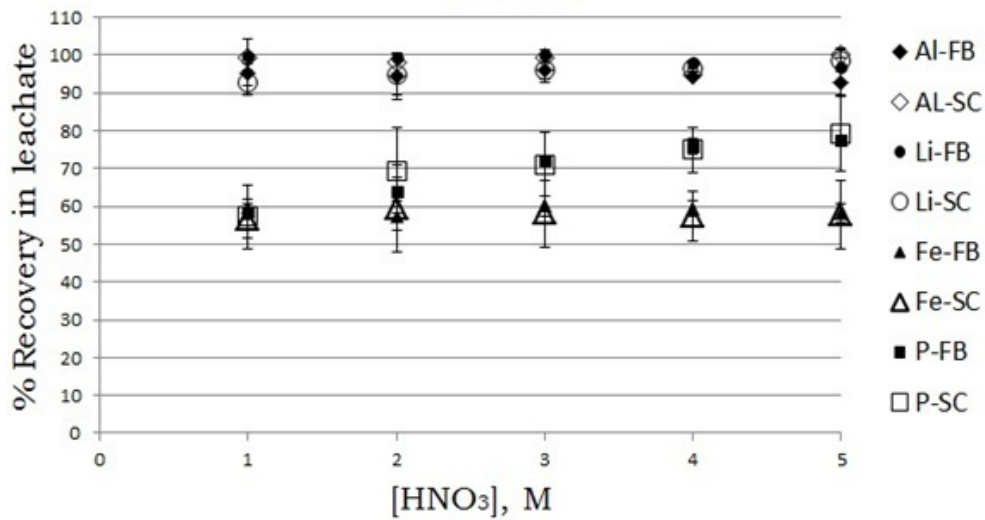


Figure 5.8. Elemental content of HNO_3 leachate FB cathode compared with that of SB at various molarities

5.3 Solvent Extraction

All solvent extraction experiments were made in duplicate to allow for uncertainty analysis. The error bars for each point on the graph, represent relative standard deviations, can be reflected as an exaggerated standard deviation values. The volume ratio was always maintained at $\Theta = 1$ and assumed so for calculation of number of stages or cycles.

5.3.1 Battery Chemistry I

In the Cyanex 272-Li-Fe chloride system (Figure 5.9), the organic phase was 0.13M Cyanex 272 in Solvent70 and the aqueous phase had 0.09M LiCl, and 0.01M of $FeCl_2 \cdot 4H_2O$. At the end of the extraction cycle1 The D_{Li} value at pH 0.1 was 11 and further was constant at 9. The Li percentage extraction was 90% at all pH values (0.1 – 1). For Fe the D_{Fe} was 0.2 at pH 0.1 and increased to 0.9 as the pH increased to 1.

On the basis of the D values the $SF_{Li/Ni}$ at pH 0.1 was 55 while at pH 1 decreased to 10. This implies that pH 0.1 – 0.2 was more suitable to separate Li from Fe in stock solution. The extraction percentage of Fe at pH 0.1 was 16%. This indicated that a single stage of extraction would not separate Li from Fe completely. The concentration of pregnant organic phase after 1 stage is about 0.08M Li and 0.008M Fe. The number of cycles necessary to get a 97% Li concentrated solution can be calculated by using equation 2.9 and was deduced to 7 cycles.

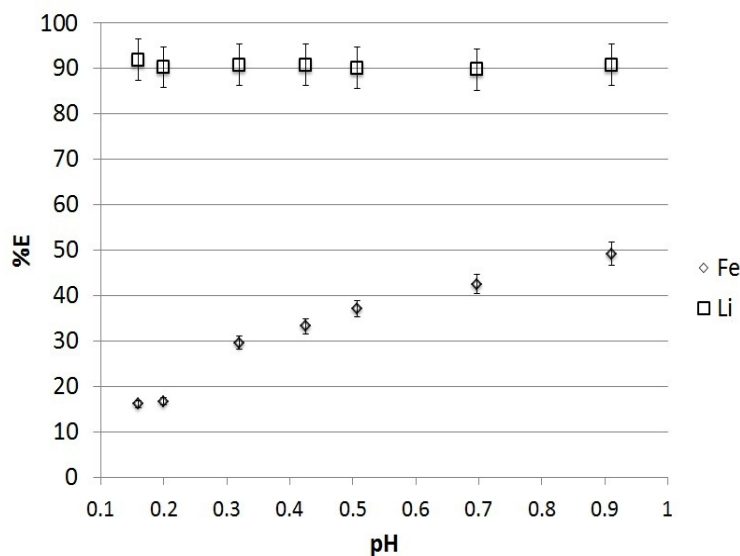


Figure 5.9. %E vs. pH in aqueous media with Li and Fe in chloride media and Organic solvent with Solvent 70 as diluent and Cyanex 272 (5%vol) as extractant

5.3.2 Battery Chemistry II

The Cyanex 272 and Li-Ni-Mn chloride system (Figure 5.10), at pH 0.7-6.8 (the pH measurements below 1 can have errors) the D_{Li} remained in the range 1.9 $\hat{\sim}$ 2.6 and the percentage extraction below pH 0.7 was of the range 4% -35%. The D_{Mn} at pH 0.7 is 1.9 and at pH 1.2 was 11.3, and steadily kept increasing to 330. The percentage extraction at pH 0.7 was 65%, and at 1.2 was 91% and reached 99% by the time the pH increased to 2. But the separation factor $SF_{Mn/Li}$ was 1 at pH 0.7, which means there was absolutely no separation. As the pH increased to 1.2 the $SF_{Mn/Li}$ was 4 which was also not a good separation. So this system is not suitable for Li and Mn separation. However Ni extraction does not start up until pH 5, so it still can be favourable to separate Ni from Mn.

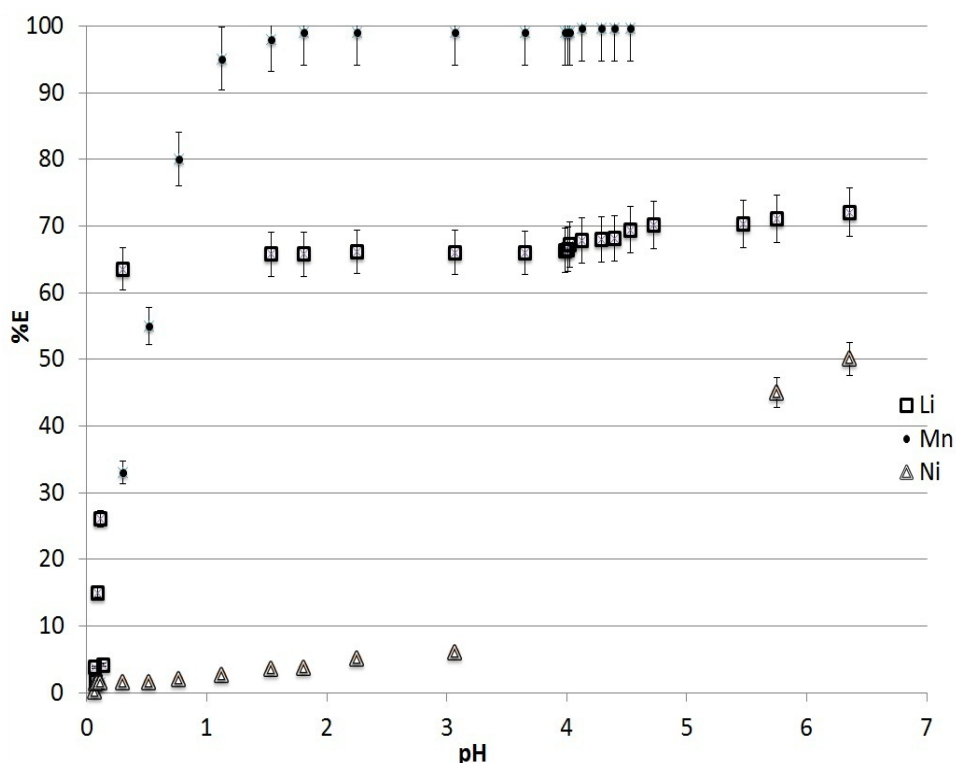


Figure 5.10. %E vs. pH in aqueous solution with *Li*, *Ni* and *Mn* in chloride media and Organic solvent with Solvent 70 as diluent and Cyanex 272 (5%vol) as an extractant

In Cyanex 272, Li-Ni-Mn in sulfate aqueous system (Figure 5.11) the D_{Li} at pH 0.5 is 0.38. The D value for Li then increases steadily with pH up until pH 2.4 where the value stabilizes at about 3.5. The percentages of extraction of Li at pH 0.4 is 28%, at pH 2.4 is 77%. The D_{Mn} value remains very low until pH 3.2 when the D_{Mn} value is 1.3 and shoots up to 12.9 at pH 4.8. The percentage extraction of Mn at pH 3.2 is 56% and at pH 4.9 is 100%. There is a good separation between Li and Mn from pH 0 to pH 2.4 although the Li extraction is only 50% the highest. Ni separation extraction starts only at $pH > 4.5$, hence the separation between Ni and the other two metals Li and Mn is reasonably good.

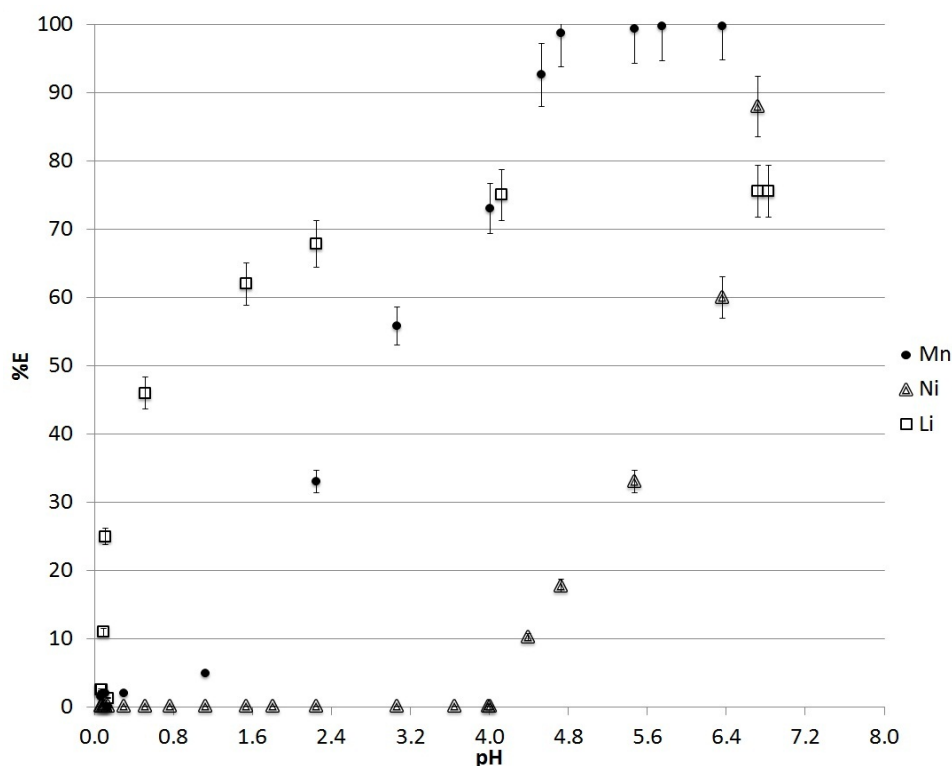


Figure 5.11. %E vs. pH in aqueous solution with *Li*, *Ni* and *Mn* in sulfate media and Organic solution with Solvent 70 as diluent and Cyanex 272 (5%vol) as an extractant

For the Cyanex923 + HDBM and Li-Ni-Mn system the D_{Li} at pH 0 is 11.7 and keeps increasing to 256 until pH 2.4 and then decreases back again (decrease not shown in figure). The Ni and Mn do not extract until $pH > 5$ and thus this system is ideal for Li separation from Mn and Ni. However the D values for both Mn and Ni above pH 5.5 are very similar making the separation between Mn and Ni impossible.

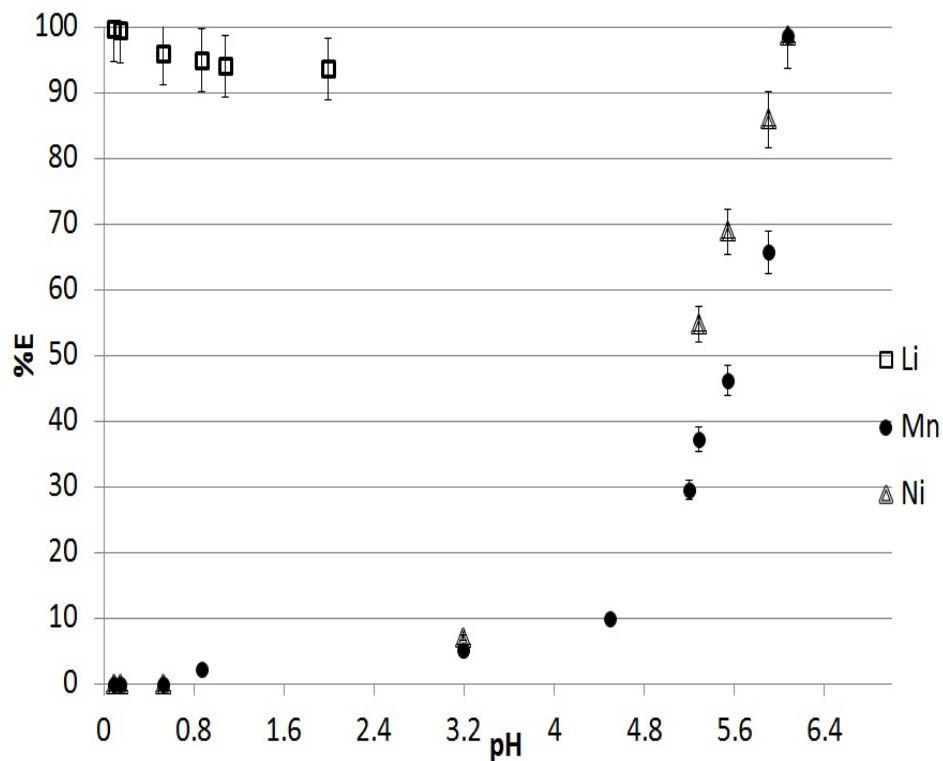


Figure 5.12. %E vs. pH in aqueous solution with *Li*, *Ni* and *Mn* in chloride media and Organic media with Xylene as diluent and Cyanex 923 (5%vol) and HDBM (0.1M) as extractants

5.4 Pyrolysis

200°C was chosen to burn away the pVdF and not oxidize the carbon. and 400°C was chosen to both burn pVdF and to completely get rid of carbon. The remaining powder from pyrolysis experiments was acid leached using three different acids (HCl , H_2SO_4 , and HNO_3). It was observed (Figure 5.13, Figure 5.14, Figure 5.15, Figure 5.16) that the remaining powder was almost free of Li. The kind of acid used for leaching did not have any considerable effect on the leaching of the remaining powder. However it should be noted the same results should not be automatically expected in the case of battery chemistry II. If a method for capturing Li is in place it may be possible to recover all the Li at as low temperature as 300°C to 400°C.

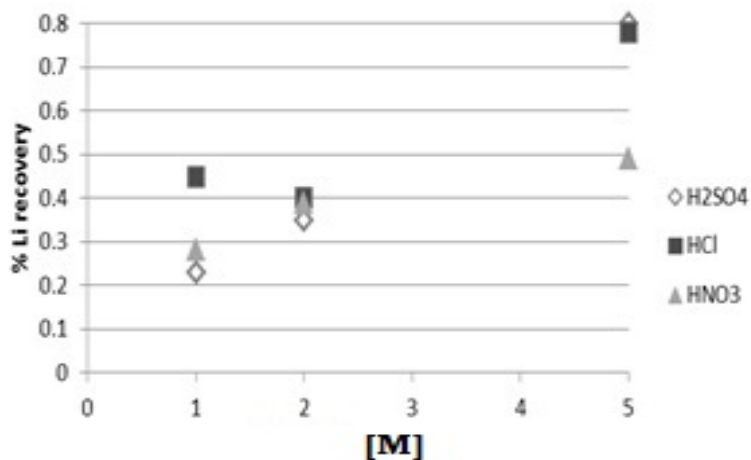


Figure 5.13. Acid leaching of the cathode sample oxidized at 200°C different molarities

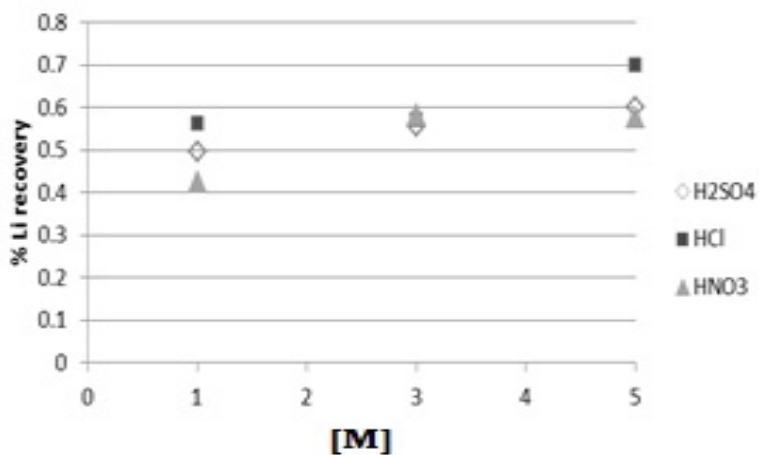


Figure 5.14. Acid leaching of the cathode sample oxidized at 400°C different molarities

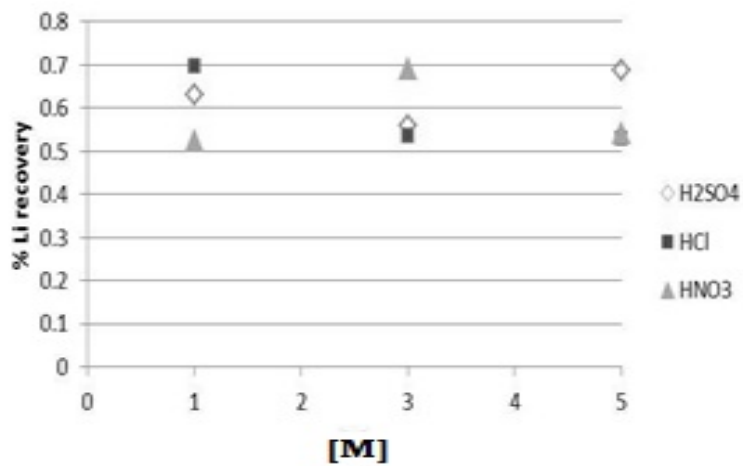


Figure 5.15. Acid leaching of the cathode sample oxidized at 500°C different molarities

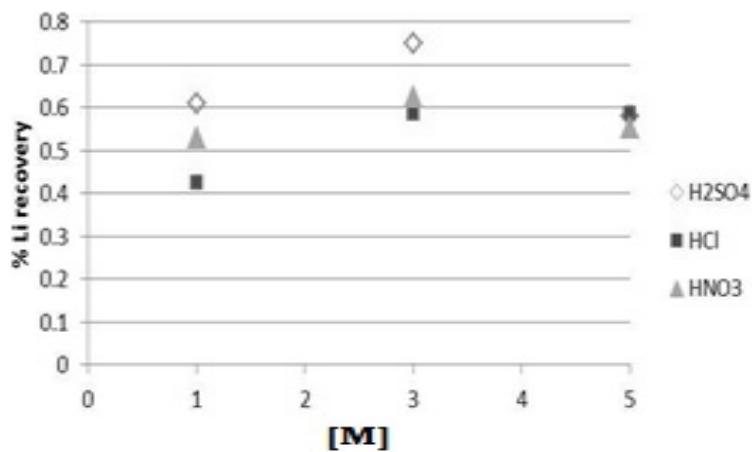


Figure 5.16. Acid leaching of the cathode sample oxidized at 600°C different molarities

5.5 Process Suggestion

Based on the leaching experiments and preliminary solvent extraction studies, the following process plan is suggested.

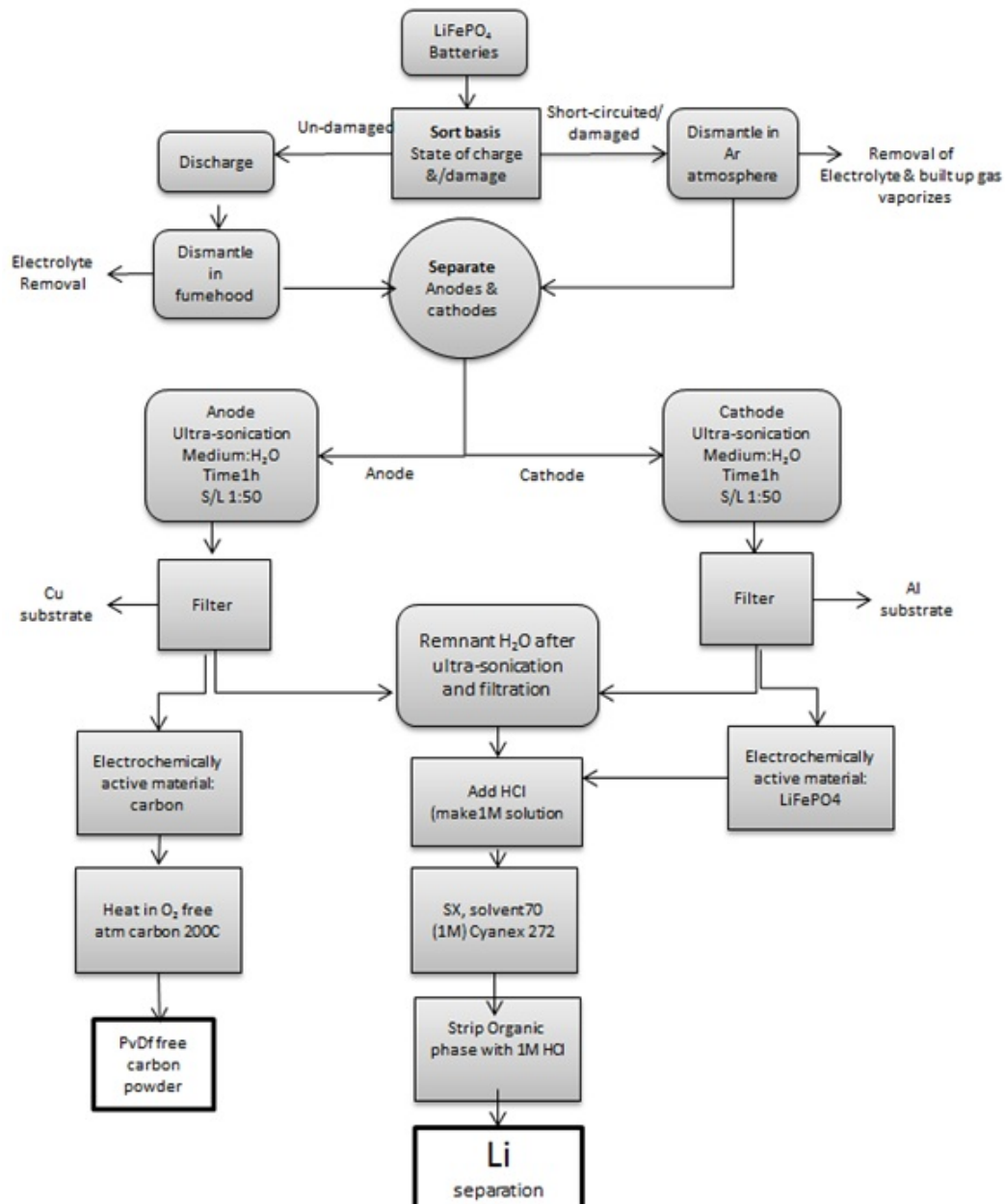


Figure 5.17. Suggested process plan

Chapter 6

Conclusions and Future Research

6.1 Conclusions

Different ELBs of the $LiFePO_4/C$ chemistry were studied with respect to the effect of their physical and charge state relative to their recyclability. The major conclusions from characterization of these batteries are that the charge and physical state though affecting the microstructure do not affect the leachability of the electrodes. Li can be leached completely from the electrodes with even moderately concentrated acids. Pure Cu and Al metal substrates can be recovered from the batteries using pure water. For this purpose separation of anodes and cathodes is necessary.

Thus preliminary results from the batch solvent extraction experiments indicate that it is possible to reach 70-90% extraction of Li using Cyanex272 with chloride media in one step. In the Li-Fe chloride aqueous system 7 cycles were suggested to get 97% Li concentrated solutions.

However, the Cyanex 272 chloride system was not very useful for Li and Mn separation, although the Ni was found to be extracted at much higher pH, hence showing good separation between Ni and the rest of the metals (Li and Mn).

The Cyanex 272 and the Li-Ni-Mn sulfate system was better compared to the chloride aqueous system because there was minimal separation between Li/Mn and Mn/Ni and good separation between Li/Ni. However the percentage extractions were not higher than 50% at the desired separation pH.

The Cyanex 923 + HDBM, the chloride-based aqueous phase was ideal for Li extraction as the Li separation was at very high acidity of the solution and much before the pH of the remaining metals extraction. However, it was not satisfactory for Mn and Ni separation as they had their D values very similar at every pH value.

Pyrolysis or high temperature oxidation experiments were not useful to recover Li mainly because the samples were devoid of Li even at as low temperatures as 200°C.

6.2 Future Research

The kinetics and temperature effect of leaching Li from cathodes will be investigated. The process suggested in this work will be followed and tested for its validity and if needed improved. Detailed solvent extraction studies, effect of extractant concentration, -ion effect (both counter and other cations) shall be investigated. Other suitable extracts shall be studied and tested. When the separation of Li is conclusively reached, purification methods such as molten salt electro-winning or precipitation will be tested.

Acknowledgments

I would like to thank the following persons and groups for their contributions to my work.

- Strykeområde Energi and Vinnova for funding my research
- My examiner Gunnar Skarnemark
- My supervisor Christian Ekberg, for giving me a great project to work with. For always giving his frank opinion about my work and for trying his best to not let me stray into strange directions. Also, for always responding to emails even after midnight and helping me with writing this thesis in an acceptable standard.
- My co-supervisor Stefan Allard, for always being kind to me and for gently nudging my transition from being a mechanical engineer to a chemical engineer. Also, for his continuous input with respect to this thesis.
- Arvid Ødegaard-Jensen, for his input on almost everything I did so far.
- Stellan, for helping me with porosity measurements, setting up my glove box and every random question I ask him.
- Teo, for helping me open my first battery.
- Robert Aronsson (ETC Battery and Fuels Cells Sweden AB), Christer Forsgren, and Bengt Steen for their ideas and informative discussions.
- Carina, for helping with my visa letters every six months.
- Kristian, for always helping me no matter what problem I came to him with and for writing such a good thesis, which will become my dictionary.
- Britt-Marie to have taken time and help me get XRD user permission.
- Anna for introducing me to EndNote, Hanna for always making sure I have my chemicals within a day I order, Elin for being there always. Thanks to all of you, and Isabelle, for being such good friends.

- Henrik, for helping me set up the furnace, and for having the most interesting conversations about science and everything else.
- Jiaxu - the only living Buddha I know of. For every piece of advice you gave me - Thank you!
- My parents, who have let me live my life even if it meant that they see me only 20 days an year.
- Abhi, what would Spock and I do without you?

Spock, if you are reading this, please don't eat it!

Bibliography

- A123-Systems (2012). <http://www.a123systems.com/lithium-ion-battery-technology.htm>.
- Bernardes, A. M., Espinosa, D. C. R. and Tenório, J. A. S. (2004). Recycling of batteries: a review of current processes and technologies, *Journal of Power Sources* **130**(1-2): 291–298. doi: DOI: 10.1016/j.jpowsour.2003.12.026.
- Bernhart, D. W., Schlick, D. T., Olschewski, D.-K. I. and Thoennes, D.-I. M. (2012). E-mobility quarterly index.
- Broussely, M., Biensan, P. and Simon, B. (1999). Lithium insertion into host materials: the key to success for li ion batteries, *Electrochimica Acta* **45**(1-2): 3–22.
- Chartrand, A. D. P. and Patrice (2001). *Thermodynamic evaluation and optimization of the LiCl-NaCl-KCl-RbCl-CsCl-MgCl₂-CaCl₂ system using the modified quasi-chemical model* **32**(6): 1361–1383.
- Chemical-Book (2012). <http://chemicalbook.com>.
- Choppin, J. R., Cox, M., Musikas, C. and R., G. (2004). *Solvent Extraction principles and practices*, 2 edn.
- Ekeremo, V. (2009). *Recycling opportunities for li-ion batteries from hybrid electric vehicles*, Master's thesis.
- Endo, M., Kim, C., Nishimura, K., Fujino, T. and Miyashita, K. (2000). Recent development of carbon materials for li ion batteries, *Carbon* **38**(2): 183–197.
- Gaines, L. (2009). Lithium-ion battery recycling issues, *Technical report*, Argonne National Laboratories.
- Gosden, D. F. (1993). Battery requirements for electric vehicles, *Journal of Power Sources* **45**(1): 61–71.

- Grosjean, C., Miranda, P. H., Perrin, M. and Poggi, P. (2012). Assessment of world lithium resources and consequences of their geographic distribution on the expected development of the electric vehicle industry, *Renewable and Sustainable Energy Reviews* **16**(3): 1735–1744.
- Inc., T. (2012). <http://www.toxco.com>.
- Karden, E., Shinn, P., Bostock, P., Cunningham, J., Schoultz, E. and Kok, D. (2005). Requirements for future automotive batteries - a snapshot, *Journal of Power Sources* **144**(2): 505–512.
- Lee, D. A., Taylor, W. L., McDowell, W. J. and Drury, J. S. (1968). Solvent extraction of lithium, *Journal of Inorganic and Nuclear Chemistry* **30**(10): 2807–2821.
- Marcus, Y. (1979). Solvent extraction chemistry. fundamentals and applications : by tatsuya sekine and yuko hasegawa, science university of tokyo, japan. marcel dekker inc., new york and basel, 1977, xii + 919 pp, *Fluid Phase Equilibria* **3**(2-3): 252–253.
- Nissan (2012). <http://www.nissanusa.com/leaf-electric-car/index>.
- Parliament, T. E. and the council of the European Union (2006). Directive 2006/66/ec.
- Patil, A., Patil, V., Wook Shin, D., Choi, J.-W., Paik, D.-S. and Yoon, S.-J. (2008). Issue and challenges facing rechargeable thin film lithium batteries, *Materials Research Bulletin* **43**(8-9): 1913–1942.
- Pistoia, G. (2009). *Areas of Battery Applications*, Elsevier, Amsterdam, pp. 1–15.
- Pistoia, G. and Gianfranco, P. (2005). *Characteristics of Batteries for Portable Devices*, Elsevier Science B.V., Amsterdam, pp. 17–27.
- Reuter, M. A., van Schaik, A., Ignatenko, O. and de Haan, G. J. (2006). Fundamental limits for the recycling of end-of-life vehicles, *Minerals Engineering* **19**(5): 433–449.
- Scrosati, B. and Garche, J. (n.d.). Lithium batteries: Status, prospects and future, *Journal of Power Sources* **195**(9): 2419–2430.
- Shin, S. M., Kim, N. H., Sohn, J. S., Yang, D. H. and Kim, Y. H. (2005). Development of a metal recovery process from li-ion battery wastes, *Hydrometallurgy* **79**(3-4): 172–181.
- Tahil, W. (2008). *The trouble with lithium*.
- Yaksic, A. and Tilton, J. E. (2009). Using the cumulative availability curve to assess the threat of mineral depletion: The case of lithium, *Resources Policy* **34**(4): 185–194.
- Zhang, W.-J. (2011). A review of the electrochemical performance of alloy anodes for lithium-ion batteries, *Journal of Power Sources* **196**(1): 13–24.